J|A|C|S
ARTICLES
Published on Web 03/24/2006

ENDOR of NO-Ligated Cytochrome *c*′

Oleg M. Usov,[†] Peter S.-T. Choi,[‡] James P. Shapleigh,[‡] and Charles P. Scholes*,[†]

Contribution from the Department of Chemistry, Center for Biochemistry and Biophysics, University at Albany, SUNY, Albany, New York 12222, and Department of Microbiology, Wing Hall, Cornell University, Ithaca, New York 14853

Received August 4, 2005; E-mail: cps14@albany.edu

Abstract: The five-coordinate NO-bound heme in cytochrome *c*′ from an overexpressing variant of denitrifying *R. sphaeroides* 2.4.3 was investigated by proton, nitrogen, and deuterium Q-band ENDOR (electron nuclear double resonance). ENDOR was a direct probe of the unpaired electron density on the nitrogen of NO and, as measured across the EPR line shape, showed a hyperfine coupling range from 36 to 44 MHz for ^{14}NO and 51 to 63 MHz for ^{15}NO. The smallest NO coupling occurred at an electronic *g*-tensor axis perpendicular to the FeNO plane, and the largest hyperfine coupling occurred in the FeNO plane where the highest nitrogen valence spin density is located. The isotropic component of the NO hyperfine coupling indicated that the electron spin on the NO is not simply in a π^* orbital having only 2*p* character but is in an orbital having 2*s* and 2*p* character in a 1:2 ratio. ENDOR frequencies from heme meso-protons, assigned with reference to porphyrin models, were determined to result from an anisotropic hyperfine tensor. This tensor indicated the orientation of the heme with respect to the FeNO plane and showed that the FeNO plane bisects the heme N−Fe−N 90° angle. ENDOR provided additional structural information through dipolar couplings, as follows: (1) to the nearest proton of the Phe14 ring, ∼3.1 Å away from the heme iron, where Phe14 is positioned to occlude binding of NO as a 6th (distal) ligand; (2) to exchangeable deuterons assigned to Arg127 which may H-bond with the proximal NO ligand.

Introduction

Nitric oxide coordinates to protein heme centers in the physiologically important processes of NO metabolism and signal transduction.[1,2] There are two general classes of ferrous NO-heme complexes, those that have a six-coordinate heme-nitrosyl with NO bound opposite to an endogenous amino acid ligand such as histidine and those that have five-coordinate heme-nitrosyl and no sixth ligand. The binding or unbinding of an endogenous amino acid is critical in controlling the reactivity of the bound NO and in controlling NO-induced conformational changes. As a notable example from soluble guanylate cyclase (SGC), five-coordinate NO-heme formation and associated Fe−His bond cleavage at the regulatory heme site trigger enzymatic activity at the guanylate cyclase enzymatic site and lead to a resultant signal cascade.[1,3] Kinetic studies have shown that the heme site of guanylate cyclase starts transiently as a NO-heme-His six-coordinate complex and kinetically progresses to five-coordinate NO-heme as the NO in the 6th position is lost and the proximal histidine at the 5th liganding position is replaced by NO.[3−8]

SGC happens to be a large eukaryotic protein which has yet to be crystallized in its entirety. In the course of NO binding, the simpler dimeric cytochrome *c*′ (Cyt *c*′), which has been crystallized, appears to go through much the same NO binding process as that of the regulatory heme site of SGC.[3,4,9−13] When NO binds to Cyt *c*′, the spectroscopic and the crystallographic evidence (Figure 1) is that the NO-bound form is five-coordinate and that the NO has replaced the former proximal histidine, leaving the 6th site opposite the NO vacant.[6,7] The NO-induced conformational change is propagated to the Cyt *c*′ dimer interface where it alters the monomer−dimer equilibrium and affects the cooperativity of NO binding.[8]

Cyt *c*′ represents the first crystallographically characterized example of a protein where an exogenous NO ligand replaces the proximal histidine to provide a five-coordinate NO-heme-protein. The expressible Cyt *c*′ which we study is from denitrifying bacteria, *R. sphaeroides* 2.4.3, which create and turn over NO in the course of denitrifying nitrite and nitrate.[14,15]

[†] University at Albany.
[‡] Cornell University.

(1) Denninger, J. W.; Marletta, M. A. *Biochim. Biophys. Acta* **1999**, *1411*, 334−350.
(2) Wasser, I. M.; de Vries, S.; Moenne-Loccoz, P.; Schroder, I.; Karlin, K. D. *Chem. Rev.* **2002**, *102*, 1201−1234.
(3) Ballou, D. P.; Zhao, Y.; Brandish, P. E.; Marletta, M. A. *Proc. Natl. Acad. Sci. U.S.A.* **2002**, *99*, 12097−12101.
(4) Zhao, Y.; Hoganson, C.; Babcock, G. T.; Marletta, M. A. *Biochemistry* **1998**, *37*, 12458−12464.
(5) Zhao, Y.; Brandish, P. E.; Ballou, D. P.; Marletta, M. A. *Proc. Natl. Acad. Sci. U.S.A.* **1999**, *96*, 14753−14758.
(6) Lawson, D. M.; Stevenson, C. E.; Andrew, C. R.; George, S. J.; Eady, R. R. *Biochem. Soc. Trans.* **2003**, *31*, 553−557.
(7) Lawson, D. M.; Stevenson, C. E.; Andrew, C. R.; Eady, R. R. *EMBO J.* **2000**, *19*, 5661−5671.
(8) Mayburd, A. L.; Kassner, R. J. *Biochemistry* **2002**, *41*, 11582−11591.
(9) Stone, J. R.; Marletta, M. A. *Biochemistry* **1994**, *33*, 5636−5640.
(10) Stone, J. R.; Sands, R. H.; Dunham, W. R.; Marletta, M. A. *Biochem. Biophys. Res. Commun.* **1995**, *207*, 572−577.
(11) Zhao, Y.; Marletta, M. A. *Biochemistry* **1997**, *36*, 15959−15964.
(12) Zhao, Y.; Schelvis, J. P.; Babcock, G. T.; Marletta, M. A. *Biochemistry* **1998**, *37*, 4502−4509.
(13) Zhao, Y.; Brandish, P. E.; DiValentin, M.; Schelvis, J. P.; Babcock, G. T.; Marletta, M. A. *Biochemistry* **2000**, *39*, 10848−10854.

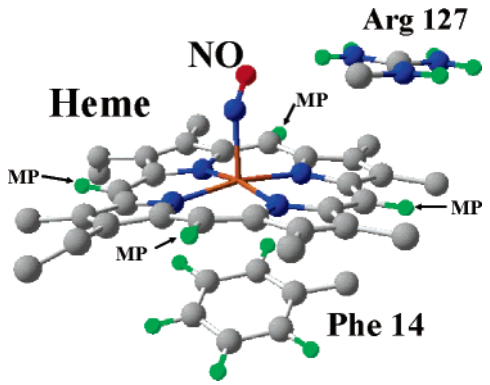

Figure 1. Schematic of the local environs of the heme group in Cyt *c*′, showing the NO, the arginine near the NO (Arg127 in *R. sphaeroides*), and the occluding Phe14 on the opposite side of the heme. The coordinates of the heme, NO, and arginine are from *A. xylosoxidans* (1E85), and the coordinates of Phe14 were superimposed from *R. sphaeroides* (1GQA) using the superposition tool of Swiss PdB Viewer. This is a composite figure created from the heme, NO, and arginine coordinates of the NO-Cyt *c*′ of *A. xylosoxidans* and the Phe14 and heme coordinates of ferric Cyt *c*′ of *R sphaeroides*; the numbering system is that of *R. sphaeroides*. Phe14 and Arg127 of *R. sphaeroides* are homologous to Leu16 and Arg124 of *A. xylosoxidans*. The protons labeled MP are the heme meso-protons. There are two crystallographically resolved orientations of the NO, and the closer one to Arg127 is shown.

It and homologous bacterial Cyts *c*′ have a function of NO transport and storage.[8,15] In contrast to the incompletely known heme locale in SGC, the substituents near the heme in Cyt *c*′ which can modulate the unusual five-coordinate NO binding are known. Figure 1 shows the heme, NO, and nearby positive arginine whose coordinates were taken from the crystal structure of NO-Cyt *c*′ of *A. xylosoxidans* (PDB file 1E85),[7] where the Cyt *c*′ that has been crystallized is a five-coordinate NO-heme complex. The histidine on the "proximal" side of the heme, which is bound to the heme in the ferric state, is replaced by NO in the ferrous NO-bound protein. Close to the NO is the highly conserved arginine (Arg127 in Figure 1) which is thought to interact with the bound NO. The FeNO plane is parallel to the direction from Fe to one of the meso-protons, and thus this plane bisects the heme N−Fe−N 90° angle. A similar orientation of the FeNO plane with respect to the heme has been found in the model ferrous octaethyl porphyrin NO complex, Fe(OEP)(NO).[16,17] In NO-Cyt *c*′ of *A. xylosoxidans* there happen to be two crystallographically resolved orientations of the NO, approximately rotated 180° from each other;[7] in Figure 1 we show the NO which is closer to the arginine. Because we are studying the homologous NO-Cyt *c*′ of *R. sphaeroides*, we use the amino acid numbering system relevant to *R. sphaeroides* in Figure 1 and provide the correlation between *R. sphaeroides* and *A. xylosoxidans* numbering in the legend to Figure 1. On the other, "distal", side of the heme plane there is a large hydrophobic group which occludes NO binding. In *R. sphaeroides* this group is Phe14, and in *A. xylosoxidans* it is Leu16. The orientation of Phe14 shown in Figure 1 was obtained by superimposing the heme and accompanying Phe14 coordinates of Cyt *c*′ of *R. sphaeroides* (PDB file 1GQA from ferric Cyt *c*′)[18] upon the heme of NO-Cyt *c*′ of *A. xylosoxidans* (PDB file 1E85) via the superposition tool of Swiss PdB Viewer. Thus Figure 1 is a composite figure created from the heme, NO, and arginine coordinates of the NO-Cyt *c*′ of *A. xylosoxidans* and the Phe14 and heme coordinates of ferric Cyt *c*′ of *R sphaeroides*.

The technique of electron nuclear double resonance (ENDOR) has been used over the last several decades to probe the electron spin density of heme iron ligands in high,[19,20] and low[21] spin ferric heme proteins, and most recently of the intermediate spin ferric Cyt *c*′ of *R. sphaeroides*.[22] For the nearest neighbor nitrogen ligands, ENDOR provided information on the valence electron spin distributions. For protons which are inherently unresolvable by X-ray crystallography, ENDOR provided evidence for the vector distance from the Fe to these protons and for weak covalent spin transfer to these protons. When paramagnetic NO binds to ferrous heme, a spin-$^1/_2$ species arises that shows shared electron density among the nitrogen of NO, the heme iron, and, when available, the liganding histidine nitrogen. To date ENDOR has been used to explore the NO derivatives of hemoglobin, myoglobin,[23−25] and cytochrome *c* oxidase,[26,27] where NO serves as an inhibitor of and mimic for dioxygen. With the exception of the five-coordinate T state hemoglobin,[28] these proteins have been six-coordinate histidine-ligated NO proteins. The ENDOR and EPR evidence showed that there was considerable electron spin density within the NO π^* orbital and covalent spin transfer to the liganding proximal histidine nitrogen.[26,28−30] ENDOR has additionally elucidated small hyperfine couplings to exchangeable and nonexchangeable protons from the neighboring amino acids, in particular, protons from proximal and distal histidine.[28,31]

NO has been found not just to be an O_2 mimic but to have intrinsic biological significance in NO-sensing, signaling, and transporting. Although ENDOR on six-coordinate NO-liganded heme proteins (where NO is an O_2 mimic) has been done with identification of NO and His nitrogen features, such measurements have not been done on a five-coordinate NO-hemeprotein of the NO-sensing, signaling, and transporting variety.[8,15] A goal of our work, for which ENDOR is uniquely suited, is to probe the intimate details of the NO-heme center, such as the detailed electronic hyperfine structure of nitrogen and protons within the NO-heme complex and to probe, through proton hyperfine

(14) Choi, P. S.-T. Insights into nitric oxide metabolism by the denitrifier *Rhodobacter sphaeroides* 2.4.3". Ph.D., Cornell, 2004.
(15) Choi, P. S.; Grigoryants, V. M.; Abruna, H. D.; Scholes, C. P.; Shapleigh, J. P. *J. Bacteriol.* **2005**, *187*, 4077−4085.
(16) Ellison, M. K.; Scheidt, W. R. *J. Am. Chem. Soc.* **1997**, *119*, 7404−7405.
(17) Hayes, R. G.; Ellison, M. K.; Scheidt, W. R. *Inorg. Chem.* **2000**, *39*, 3665−3668.
(18) Ramirez, L. M.; Axelrod, H. L.; Herron, S. R.; Rupp, B.; Allen, J. P.; Kantardjieff, K. A. *Journal of Chemical Crystallography* **2003**, *33*, 413−424.
(19) Scholes, C. P. ENDOR on Hemes and Hemoproteins. In *Multiple Electron Resonance Spectroscopy*; Dorio, M., Freed, J. H., Eds., Plenum Press: New York, 1979; pp 297−329.
(20) Scholes, C. P.; Lapidot, A.; Mascarenhas, R.; Inubushi, T.; Isaacson, R. A.; Feher, G. *J. Am. Chem. Soc.* **1982**, *104*, 2724−2735.
(21) Scholes, C. P.; Falkowski, K. M.; Chen, S.; Bank, J. *J. Am. Chem. Soc.* **1986**, *108*, 1660−1671.
(22) Usov, O. M.; Choi, P. S.-T.; Shapleigh, J. P.; Scholes, C. P. *J. Am. Chem. Soc.* **2005**, *127*, 9485−9494.
(23) Dickinson, L. C.; Chien, J. C. *J. Am. Chem. Soc.* **1971**, *93*, 5036−5040.
(24) Dickinson, L. C.; Chien, J. C. *Biochem. Biophys. Res. Commun.* **1974**, *59*, 1292−1297.
(25) Hori, H.; Ikeda-Saito, M.; Yonetani, T. *J. Biol. Chem.* **1981**, *256*, 7849−7855.
(26) LoBrutto, R.; Wei, Y. H.; Mascarenhas, R.; Scholes, C. P.; King, T. E. *J. Biol. Chem.* **1983**, *258*, 7437−7448.
(27) LoBrutto, R.; Wei, Y. H.; Yoshida, S.; Van Camp, H. L.; Scholes, C. P.; King, T. E. *Biophys. J.* **1984**, *45*, 473−479.
(28) Hüttermann, J.; Burgard, C.; Kappl, R. *J. Chem. Soc., Faraday Trans.* **1994**, *90*, 3077−3087.
(29) Hohn, M.; Hüttermann, J.; Chien, J. C. W.; Dickinson, L. C. *J. Am. Chem. Soc.* **1983**, *105*, 109−115.
(30) Kappl, R.; Hüttermann, J. *Israel Journal of Chemistry* **1989**, *29*, 73−84.
(31) Flores, M.; Wajnberg, E.; Bemski, G. *Biophys. J.* **2000**, *78*, 2107−2115.

couplings, the orientation of nearby amino acid residues which influence the mode of NO binding. The work started here is on the simpler and bacterially expressible Cyt *c′*. These studies are intended to provide benchmarks for a subsequent probe of perturbations, such as those brought on by mutating amino acids near the heme, that will provide insight into the NO-binding process. They are also intended to provide experimental electronic structural and hyperfine parameters for comparison with parameters generated by density functional theory (DFT).[32,33]

Methods and Materials

Materials. Methods for overexpressing and purifying Cyt *c′* from the denitrifying *R. sphaeroides* 2.4.3 are described by Choi et al.[15] and Usov et al.[22] The methods for the his-tagged version of Cyt *c′* are given in the body of the paper by Usov et al.,[22] and the methods for the non-his-tagged version are given in its Supporting Information. The detailed sequences and a comparison to the sequence from a closely related Cyt *c′* of *R. sphaeroides* R26 which has provided the most relevant crystal structure to the system studied, albeit in its ferric form,[18] are given in the Supporting Information of Usov et al.[22] The EPR spectra and proton and nitrogen ENDOR spectra from the mixed-spin ferric versions of non-His-tagged Cyt *c′* and His-tagged Cyt *c′* were nearly identical.[22]

^{14}NO of 99% chemical purity was purchased from Air Products, and ^{15}NO of >98% isotopic enrichment and purity was purchased from Cambridge Isotopes. NADH (Sigma) was used as a reductant, and phenazine methosulfate (Sigma), as redox mediator. NO gas at 1 atm pressure, scrubbed through concentrated pH 7 phosphate buffer, was anaerobically withdrawn into 5 mL Hamilton syringes that had been preflushed with argon. ENDOR samples of Cyt *c′* intended to have a final 50 μL volume were initially concentrated to approximately 1 mM in heme in pH 7.0, 0.05 M phosphate buffer; these samples contained 50% glycerol by volume to favor glass formation. (For deuteration, the samples were exchanged twice versus D_2O buffer at pD 7 to an approximate 95% D_2O enrichment, and perdeuterated glycerol was used as a glassing agent.) Samples containing 10 μM phenazine methosulfate were flushed by scrubbed argon gas for at least 5 min in a 10 mL septum-stoppered vial. Then argon-deaerated NADH reductant in 4-fold molar excess with respect to heme protein was added, and 3 mL of NO gas were added to the vial. After allowing the reaction to occur for approximately 1 min, the NO-Cyt *c′* was withdrawn with a Hamilton gastight syringe, transferred under argon to ENDOR tubes, and frozen under argon by plunging into liquid nitrogen. Sperm whale myoglobin (Mb) samples (Boeringer Mannheim) were similarly prepared in pH 6 (or pD 6) MES at a concentration of approximately 3 mM[26] and similarly frozen in glycerol. Samples of Fe(OEP)(NO) (octaethylporphyrin) and Fe(TPP)(NO) (tetraphenylporphyrin), 1 mM in concentration, were prepared by reductive nitrosylation of the appropriate Fe(OEP)Cl or Fe(TPP)Cl (Strem Chemical) in a 1:1 chloroform/methylene chloride mixture and a small amount of methanol.[34,35] The ENDOR tubes were precision 2.0 mm i.d. (inside diameter), 2.4 mm o.d. (outside diameter) sample tubes (Vitrodynamics, Rahway, NJ).

Methods. EPR-ENDOR Spectroscopic Methods. X-band EPR (9.52 GHz) was carried out under those cryogenic conditions described previously for mixed spin ferric Cyt *c′*.[22] EPR spectra were simulated by application of the simulation/fitting routine SIMPIPM.[36] Q-band (34.1 GHz) ENDOR measurements were performed under dispersion (χ'), rapid passage, field-modulated conditions with a cryogenically tunable TE_{011} Q-band resonator[37] at 2 K as previously reported.[38−40] In doing ENDOR, we monitor the radio frequency (RF)-induced change in the rapid-passage, 100 kHz field modulated dispersion EPR signal as we sweep the frequency of the RF field. Through previous experience we have determined that strongly coupled protons (coupling ≥ 4 MHz), and nitrogens are best resolved with a higher field modulation ≥ 1 G ptp (peak-to-peak) while weakly coupled nuclei including protons and deuterons are best resolved with smaller field modulation ≤ 0.5 G ptp.[22] Since rapid passage ENDOR signals may be distorted in the direction of the frequency sweep by internal spin relaxation, we find it useful to obtain the average frequencies of the broader proton and nitrogen ENDOR features[22] by separate sets of frequency sweeps, first in an upward and then in a downward direction.

ENDOR Theory − Protons. The frequencies of proton ENDOR features, $^{P}\nu_{ENDOR}$, center to first order at the free proton nuclear Zeeman frequency, ν^P. Taking A as the hyperfine coupling, one finds the frequencies are split away from ν^P by $\pm^1/_2A$ for protons coupled to the electron spin $^1/_2$ doublet. Proton ENDOR frequencies, occurring as "+" or as "−" Zeeman branches, are[41]

$$^{P}\nu^{\pm}_{ENDOR} = |\nu^P \pm A/2| \qquad (1)$$

First-order expressions hold when $\nu^P \gg A/2$, as is the case here with a magnetic field of ∼1.2 T and ν^P in the 50 MHz range. Under rapid passage conditions the intensity of the "+" and the "−" branches need not be the same;[38,39,41,42] (Fortunately, the major information from ENDOR is in the frequency of features from which hyperfine couplings are derived and not in the ENDOR intensities whose details may be affected by spin relaxation and RF and microwave power levels.)

To explain proton electron hyperfine coupling we refer to the Spin Hamiltonian formalism explained by Carrington and McLachlan,[43] Chapter 7, in which the electron nuclear hyperfine interaction is written as **S·A·I**, where **S** is the electron spin operator, **I** is the nuclear spin operator, and **A** is the electron−nuclear hyperfine tensor. The hyperfine interaction consists of an isotropic part, a_{iso}**S·I**, arising from a Fermi contact interaction, and an anisotropic, traceless part, **S·T·I**, due to the electron nuclear dipolar interaction.

$$\mathbf{S{\cdot}A{\cdot}I} = A_1S_1I_1 + A_2S_2I_2 + A_3S_3I_3 = a_{iso}\mathbf{S{\cdot}I} + \mathbf{S{\cdot}T{\cdot}I} \qquad (2)$$

$$\text{where } \mathbf{A} = a_{iso}\mathbf{E} + \mathbf{T} \text{ (}\mathbf{E}\text{ is the unity matrix)}$$

$$A_1 = a_{iso} + T_1$$

$$A_2 = a_{iso} + T_2$$

$$A_3 = a_{iso} + T_3$$

a_{iso} is the average of A_1, A_2, and A_3, and $(T_1 + T_2 + T_3) = 0$. The principal axes of the anisotropic hyperfine tensor are 1, 2, and 3, where the axis labeled "3" is the axis for largest hyperfine coupling.

As elaborated in the Discussion, the protons on the periphery of the heme group may have small covalent contributions to their contact and

(32) Zhang, Y.; Gossman, W.; Oldfield, E. *J. Am. Chem. Soc.* **2003**, *125*, 16387−16396.
(33) Zeng, Z.; Guenzburger, D.; Ellis, D. E. *THEOCHEM* **2004**, *678*, 145−156.
(34) Gilbert, D. C.; Doetschman, D. C. *Chemical Physics* **2001**, *269*, 125−135.
(35) Scheidt, W. R.; Frisse, M. E. *J. Am. Chem. Soc.* **1975**, *97*, 17−21.
(36) SIMPIPM is an extension of PIP which is an extension of QPOW. Nilges, M. J., Belford, R. L., and Francesconi, L. C. Simulation of strain in EPR spectra using the method of gradients; 40th Rocky Mountain Conference on Analytical Chemistry, Denver, Colorado, July 1998. For QPOW, see: Nilges, M. J., Thesis, University of Illinois, Urbana, 1979.
(37) Sienkiewicz, A.; Smith, B. G.; Veselov, A.; Scholes, C. P. *Rev. Sci. Instrum.* **1996**, *67*, 2134−2138.
(38) Veselov, A.; Olesen, K.; Sienkiewicz, A.; Shapleigh, J. P.; Scholes, C. P. *Biochemistry* **1998**, *37*, 6095−6105.
(39) Veselov, A. V.; Osborne, J. P.; Gennis, R. B.; Scholes, C. P. *J. Am. Chem. Soc.* **2000**, *122*, 8712−8716.
(40) Zhao, Y.; Lukoyanov, D. A.; Toropov, Y. V.; Wu, K.; Shapleigh, J. P.; Scholes, C. P. *Biochemistry* **2002**, *41*, 7464−7474.
(41) Hoffman, B. M.; DeRose, V. J.; Doan, P. E.; Gurbiel, R. J.; Houseman, A. L. P.; Telser, J. In *Biological Magnetic Resonance*, *Vol. 13: EMR of Paramagnetic Molecules*; Berliner, L. J., Reuben, J., Eds.; Plenum: New York, 1993; Vol. 13.
(42) Werst, M. M.; Davoust, C. E.; Hoffman, B. M. *J. Am. Chem. Soc.* **1991**, *113*, 1533−1538.
(43) Carrington, A.; McLachlan, A. D. *Introduction to Magnetic Resonance with Applications to Chemistry and Chemical Physics*; Harper & Row: New York, 1967.

dipolar interactions from electron spin transferred through the porphyrin from the metal,[22] but in addition they have larger dipolar couplings to electron spin localized on the metal. Outlying, noncovalently linked protons such as those on Phe14 or Asp127 will typically only have dipolar couplings with electron spin localized near the iron.

The dipolar coupling to spin localized on the iron is explained by point dipolar coupling, for which the magnitude is

$$A_{\mathrm{PTdip}}(3\cos^2\theta - 1) = (f_{\mathrm{Fe}} g_{\mathrm{eff}} g_{\mathrm{n}} \beta_e \beta_n / hR^3)(3\cos^2\theta - 1)$$

$$A_{\mathrm{PTdip}} = (f_{\mathrm{Fe}} g_{\mathrm{eff}} g_{\mathrm{n}} \beta_e \beta_n / hR^3) = (39.5\, f_{\mathrm{Fe}} g_{\mathrm{eff}} / R^3)\ (\mathrm{MHz}) \qquad (3)$$

where f_{Fe} is the fraction of an unpaired electron on the iron, g_{eff} is the electronic g-value where the dipolar interaction is measured, g_{n} is the nuclear g-value (= 5.585 for a proton). **R** is the metal-to-proton vector, R is the iron−proton distance, and θ is the angle between the vector **R** and the external magnetic field. When the electronic g-anisotropy is low, as it is for the heme-NO system, the point dipolar Hamiltonian will be axial with respect to the **R** direction.

If there is significant spin density on the NO, then separate point dipolar expressions involving separate fractions of spin on the N or O might have to be summed together with the iron contribution to provide the overall dipolar spin tensor. For help in assigning ENDOR features for dipolar-coupled protons, proton positions have been inferred from PDB data where the placement of protons is either by Swiss PDB Viewer or through the rectification tool of CS Chem 3D PRO.

Nitrogen ENDOR Frequencies and Hyperfine Analyses. The first-order expressions for spin 1 ^{14}N ENDOR frequencies for heme, histidine, and NO are

$$^{14}\nu^{+}_{\mathrm{ENDOR}} = |^{14}A/2 \pm {}^{3}/_{2}P + {}^{14}\nu| \text{ and}$$
$$^{14}\nu^{-}_{\mathrm{ENDOR}} = |^{14}A/2 \pm {}^{3}/_{2}P - {}^{14}\nu| \quad (4)$$

where ^{14}A is the hyperfine coupling, P is the quadrupolar coupling, and $^{14}\nu$ (= 3.75 MHz at 1.218 T) is the ^{14}N nuclear Zeeman frequency. (If quadrupolar splitting is resolved, the quadrupolar splitting will be $3|P|$.) The first-order expressions for spin $^{1}/_{2}$ ^{15}N ENDOR frequencies are

$$^{15}\nu^{+}_{\mathrm{ENDOR}} = |^{15}A/2 + {}^{15}\nu| \text{ and } {}^{15}\nu^{-}_{\mathrm{ENDOR}} = |^{15}A/2 - {}^{15}\nu| \quad (5)$$

where ^{15}A is the hyperfine coupling, $P = 0$, and $^{15}\nu$ (= 5.25 MHz at 1.218 T) is the ^{15}N nuclear Zeeman frequency. For either ^{14}N or ^{15}N nitrogen here, as opposed to protons, the hyperfine term, $A/2$, outweighs the other terms. At Q-band the nitrogen ENDOR features typically occur with frequencies below 40 MHz (i.e., A < 80 MHz), while the proton ENDOR features are all above 50 MHz and are well separated from nitrogen ENDOR. The $^{14}\nu^{+}_{\mathrm{ENDOR}}$ branch is often the only one observable with rapid passage Q-band ENDOR for nitrogen features from heme and histidine with couplings less than 30 MHz.[22,39] The hyperfine couplings to ^{14}NO and ^{15}NO are typically larger than 40 MHz, and in the cases reported here, both Zeeman partners appeared where the splitting between Zeeman partners, indicated by arrows in Figures 3 and 4, is, respectively, $2^{14}\nu$ or $2^{15}\nu$.

Results

EPR Results. Figure 2A and B, respectively, show X-band EPR spectra of ^{14}NO-Cyt c' and ^{15}NO-Cyt c', and Figure 2C and D, respectively, show the X-band EPR spectra of the ^{14}NO-Mb and ^{15}NO-Mb. The direct EPR details of hyperfine couplings to NO are better shown at the more commonly used X-band frequencies where the line width spread due to g-value anisotropy and possibly g-strain (both dependent on the EPR frequency) is less. For Cyt c', the NO hyperfine splitting near $g = 2.00$ is 16.0 ± 1.0 G (= 45.3 ± 2.8 MHz) for ^{14}NO and 23.7 ± 1.0 G (= 66.0 ± 2.8 MHz) for ^{15}NO. The hyperfine coupling to the NO is less well resolved for NO-Mb, as was obvious from previously reported spectra.[23−25,29,30,44] X-band EPR has indicated couplings of 58 and 76 MHz, respectively, to ^{14}NO-Mb and to ^{15}NO-Mb.[26] Because of its higher EPR frequency Q-band EPR (Figure 2E) of NO-Cyt c' provides a better estimate of g-values, g_{max}, g_{inter}, g_{min} = 2.116, 2.017, 2.008 (± 0.002). Five-coordinate NO-Cyt c′ has a maximal g-value of about 2.12 and a minimal g-value greater than 2.00 while six-coordinate NO-Mb has a maximal g-value of 2.07 and a minimal g-value below 2.00 of about 1.98. NO-Mb may actually contain two species having their minimal g-value below 2.00.[44]

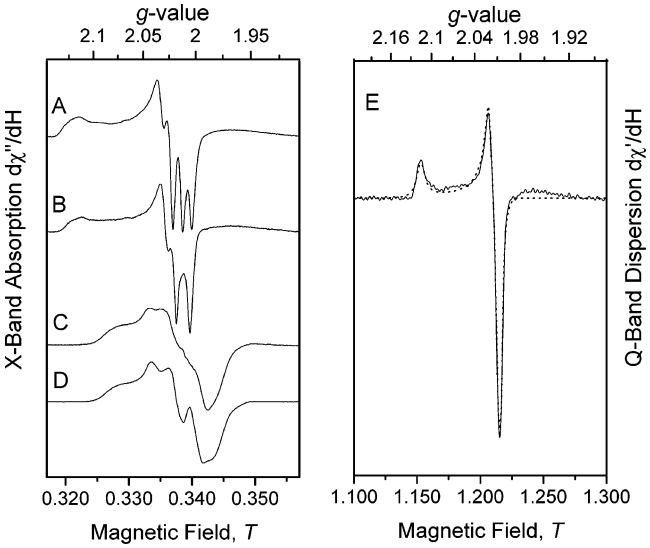

Figure 2. X-band EPR spectra of (A) ^{14}NO and (B) ^{15}NO derivatives of Cyt c' and (C) the ^{14}NO and (D) ^{15}NO derivatives of Mb. The spectra were recorded at T = 15 K, 3 G field modulation, 100 s of signal averaging with a 0.400 T sweep, 2 mW microwave power, EPR frequency ν_{EPR} = 9.525 GHz. (E) A first derivative of Q-band dispersion EPR spectrum of ^{14}NO-Cyt c' obtained at T = 2 K, 1 G field modulation, 200 s of signal averaging with a 0.200 T sweep, 0.24 μW microwave power, EPR frequency ν_{EPR} = 34.10 GHz. The dashed line shows an SIMPIPM fit to the derivative EPR line shape with g_{max} = 2.116, g_{inter} = 2.017, g_{min} = 2.008.

Nitrogen ENDOR Results. ENDOR provided evidence for nitrogen hyperfine coupling to the NO ligand, to the heme nitrogen, and, when available, to the 6th ligand, a nitrogen of the proximal histidine. (Unless otherwise indicated, NO-Cyt c′ spectra were from Cyt c' without his-tag.) For Cyt c' Figure 3, spectra A−H, taken over the g-value range from 2.122 (H = 1.148 T) to g = 2.010 (H = 12.12 T), showed excellent resolution of the ^{14}NO hyperfine coupling and provided evidence for a ^{14}NO quadupolar splitting of $3|P| = 1.95 \pm 0.3$ MHz ($|P| = 0.65 \pm 0.1$ MHz) at the low field extremum. ENDOR of ^{14}NO and ^{15}NO showed both ν^{+}_{ENDOR} and ν^{-}_{ENDOR} features and the appropriate Zeeman splittings of $2^{14}\nu$ or $2^{15}\nu$. The average ^{14}NO hyperfine coupling obtained from the frequency of the two Zeeman partners increased monotonically with increasing magnetic field and decreasing g-value. The ^{14}NO hyperfine coupling increased by about 24% from 35.7 to 43.7 MHz over the g-value range from 2.117 to 2.008, and the corresponding ^{15}NO coupling increased from 51.4 to 63.2 MHz. The largest value of the hyperfine coupling at the high field extremum agreed within experimental error with the value measured directly by EPR (Figure 2A and B) at the high field extremum

(44) Flores, M.; Wajnberg, E.; Bemski, G. *Biophys. J.* **1997**, *73*, 3225−3229.

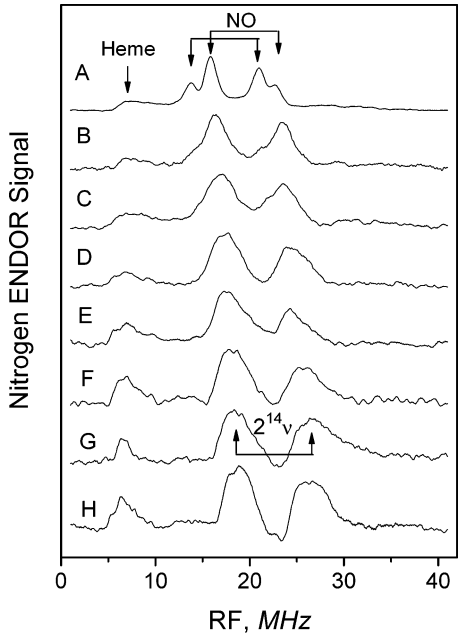

Figure 3. Nitrogen ENDOR is shown for ^{14}NO-Cyt *c′* at the following magnetic fields: 1.148 T ($g = 2.122$) (A), 1.158 T ($g = 2.104$) (B), 1.168 T ($g = 2.086$) (C), 1.178 T ($g = 2.069$) (D), 1.188 T ($g = 2.052$) (E), 1.198 T ($g = 2.034$) (F), 1.208 T ($g = 2.018$) (G), and 1.212 T ($g = 2.010$) (H). The conditions for data collection were as follows: adiabatic rapid passage, $T = 2$ K, microwave power = 0.22 nW, 100 kHz field modulation = 5 G ptp, a system time constant = 160 ms, radio frequency power ≈ 20 W, radio frequency sweep rate = 2 MHz/s, overall signal averaging time = 400 s, $\nu_{EPR} = 34.10$ GHz. Radio frequency power was pulsed with a 100/900 μs duty cycle.

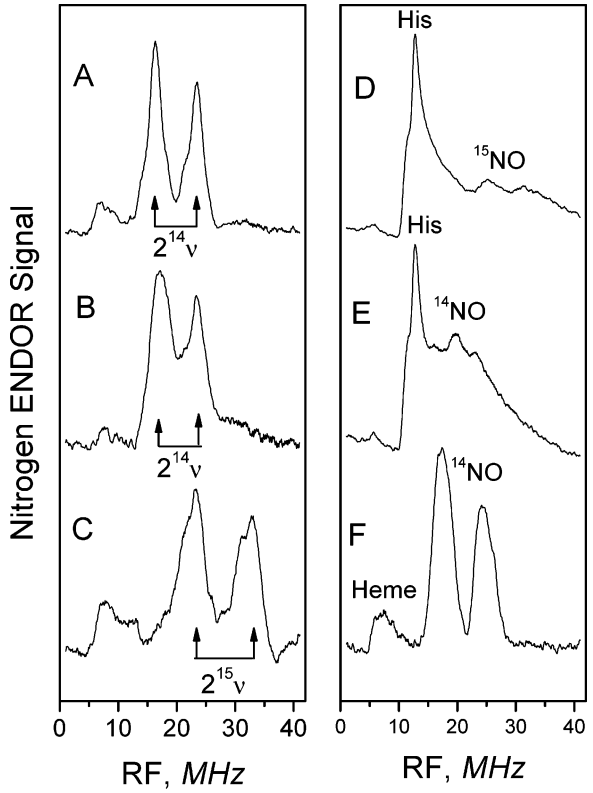

Figure 4. Spectra A−C compare nitrogen ENDOR from ^{14}NO-Cyt *c′* without his-tag (A), ^{14}NO-Cyt *c′* with his-tag (B), and ^{15}NO-Cyt *c′* without his-tag (C), all taken at 1.158 T ($g = 2.104$) which is near the low field end of the NO-Cyt *c′* EPR spectrum. Spectra D−F compare nitrogen ENDOR from ^{15}NO-Mb (D), ^{14}NO-Mb (E), and ^{14}NO-Cyt *c′* (F) at 1.178 T ($g = 2.069$), which is near the low field end of the NO-Mb EPR spectrum. The conditions for data collection were same as those in Figure 3.

of the X-band spectrum. In the ENDOR spectra of NO-Cyt *c′* there consistently were less intense features near 6 MHz, and these features evolved into one peak at the high field extremum near $g = 2.01$ (Figure 3G). The ENDOR spectral region near 6 MHz is one where weakly coupled nitrogens would be found; indeed, for protonated samples there are no other potential features than nitrogen features found in this region.

Figure 4, spectra A−C, compare the well-resolved features from near the low field extremum of ^{14}NO-Cyt *c′* (without his-tag), ^{14}NO-Cyt *c′* (his-tagged), and ^{15}NO-Cyt *c′* (without his-tag). The comparison of the ^{14}NO ENDOR from protein without his-tag to that of his-tagged ^{14}NO protein simply showed a larger ^{14}NO ENDOR line width for the his-tagged version. The ^{15}NO-Cyt *c′* ENDOR features reflected the 40% larger nuclear *g*-value for ^{15}N. In the Supporting Information (Figure 1S) a comparison of nitrogen ENDOR from ^{14}NO-Cyt *c′* to Fe(OEP)(NO) in frozen organic solvent is provided where the ENDOR features occur in the same frequency range for both five-coordinate complexes, but with better resolution for the ^{14}NO-Cyt *c′*. In Figure 1S the ENDOR frequencies from the ^{14}NO of Fe(OEP)(NO) appear approximately 1.5 MHz higher than from ^{14}NO-Cyt *c′*, implying a ^{14}NO hyperfine ~3 MHz higher for Fe(OEP)(NO).

The major additional feature observed for the NO-Mb samples, shown in Figure 4D and E and taken at a field of 1.178 T near the low field extremum for NO-Mb, is an intense ENDOR feature near 12 MHz. If assigned as the ν^+_{ENDOR} peak of a ^{14}N nitrogen, this feature has a hyperfine coupling of about 16 MHz, which is the coupling previously measured at X-band for histidine nitrogen of NO-Mb.[26] The 1.5 MHz splitting of this feature also agrees with the quadrupolar coupling ($|P| =$ 0.5 MHz) expected from histidine nitrogen. The NO ENDOR features of both ^{15}NO-Mb (Figure 4D) and ^{14}NO-Mb (Figure 4E) were considerably broader than the corresponding NO features of NO-Cyt c′ (Figure 4F) without resolution of the ν^+_{ENDOR} and ν^-_{ENDOR} pairs. NO hyperfine couplings to ^{14}NO-Mb and to ^{15}NO-Mb near $g = 2.08$ were previously measured by X-band ENDOR as 27.7 and 36.6 MHz, respectively, while the largest hyperfine couplings reported by EPR near $g = 2.00$ are, respectively, 58 and 76 MHz for ^{14}NO-Mb and ^{15}NO-Mb.[26] The 200% NO hyperfine anisotropy is considerably larger for the six-coordinate NO of NO-Mb than is the 25% NO hyperfine anisotropy for the five-coordinate NO-Cyt *c′*. Table 1 provides a comparison of nitrogen hyperfine couplings determined by EPR and ENDOR for heme nitrosyls with five-coordination [NO-Cyt *c′* and Fe(OEP)(NO) with six-coordination *a3*-NO of cytochrome oxidase and MbNO].

Proton ENDOR Results. A. Weakly Coupled Protons. For NO-Cyt *c′* there were nonexchangeable, weakly coupled proton ENDOR features within ~ ±1.5 MHz of ν^P as shown in Figure 5. The best resolved occurred at the low and high field *g*-value extremes, Figure 5A and G, respectively. At the maximal *g*-value ($g = 2.122$, $H = 1.148$ T) two outlying peaks with couplings of magnitude 1.9 (**a,a′**) and 1.5 (**b,b′**) MHz were revealed. Near the high field extremum ($g = 2.018$, $H = 1.208$ T) a set of peaks (**c,c′**) with couplings of 1.2 MHz have emerged (Figure 5F), and at the highest field (Figure 5G) additional shoulders (**d,d′**) with a splitting of 1.5 MHz have appeared. We strongly suspected that all of these foregoing protons were meso-

Table 1. NO and Histidine Nitrogen Hyperfine Couplings

Five-Coordinate NO-Heme Systems			
complex	couplings (MHz)	method	reference
Cyt *c*′-NO		ENDOR	this work
	NO $^{14}A_{min} = 35.7 \pm 0.6$	($g = 2.122$)	
	NO $^{14}A_{max} = 43.7 \pm 0.6$	($g = 2.010$)	
		ENDOR	
	NO $^{15}A_{min} = 51.4 \pm 0.6$	($g = 2.122$)	
	NO $^{15}A_{max} = 63.2 \pm 0.6$	($g = 2.010$)	
		EPR	
	NO $^{14}A_{max} = 45.3 \pm 2.8$	($g = \sim 2.010$)	
	NO $^{15}A_{max} = 66.0 \pm 2.8$		
FeOEP(NO)		EPR	ref 17
	NO $^{14}A_y = 42.5$	($g = 2.110$)	
	NO $^{14}A_x = 52.8$	($g = 2.040$)	
	NO $^{14}A_z = 44.1$	($g = 2.012$)	

Six-Coordinate NO-Heme Systems			
complex	couplings (MHz)	method	reference
NO-ferrocytochrome *a3*	NO $^{14}A_y = 30.56 \pm 0.10$	ENDOR	ref 26
	NO $^{15}A_y = 42.4 \pm 0.25$	($g = 2.086$)	
	His $^{14}A_y = 16.5 \pm 0.1$		
	NO $^{14}A_{max} = 59.9 \pm 1$	EPR	
	NO $^{15}A_{max} = 83.4 \pm 2$	($g = \sim 2.00$)	
	His $^{14}A_{max} = 19.3 \pm 1$		
	NO $^{15}A_x = 42.2 \pm 0.6$	ENDOR	
	His $^{14}A_x = 16.1 \pm 0.1$	($g = 1.97$)	
NOMb	NO $^{14}A_y = 27.7 \pm 0.3$	ENDOR	ref 26
	NO $^{15}A_y = 36.6 \pm 0.6$	($g = 2.086$)	
	His $^{14}A_y = 15.9 \pm 0.2$		
	NO $^{14}A_{max} = 56.0 \pm 1.5$	EPR	
	NO $^{15}A_{max} = 78.4 \pm 1.4$	($g = \sim 2.005$)	
	His $^{14}A_{max} = 18.5 \pm 1.5$		
		ENDOR	
	NO $^{15}A_x = 47.0 \pm 2.0$	($g = 1.969$)	

protons, which are the closest protons on the porphyrin periphery to the iron and would have the largest dipolar coupling. For comparison to the relevant NO-Cyt c′ proton spectra, proton ENDOR spectra of the five-coordinate Fe(OEP)(NO) model having meso-protons, and the Fe(TPP)(NO) model lacking meso-protons were recorded. The comparison of weakly coupled proton features from NO-Cyt *c*′, Fe(OEP)(NO) and Fe(TPP)-(NO) is shown at the high and low *g*-value extremes (Figures 5 H,H′,H″ and I,I′,I″). At comparable *g*-values the outlying proton features belonging to Fe(OEP)(NO), which are not found for Fe(TPP)(NO) and belong to heme meso-protons, were similar to outlying features from NO-Cyt *c*′ albeit, as shoulders, somewhat more poorly resolved.

B. Strongly Coupled Protons. Figures 6A−D compare across the EPR line shape the strongly coupled proton features from NO-Cyt *c*′. The couplings for these features are >2 MHz and indicate that the largest, best resolved couplings were at the highest field (lowest *g*-value) extremum. These well resolved features, labeled α,α′, had a maximal coupling of about 4.8 MHz, and they persisted in deuterated solvent, as shown by the comparison of Figure 6A−D (protonated) with Figure 6A′−D′ (deuterated). However, spectra taken in protonated solvent did appear on comparison to the corresponding deuterated spectra to have additional broad underlying ENDOR intensity. Attempts were made to resolve the corresponding exchangeable deuterium ENDOR, and the deuterium ENDOR spectrum is provided in the inset to Figure 6. The deuterium spectrum was

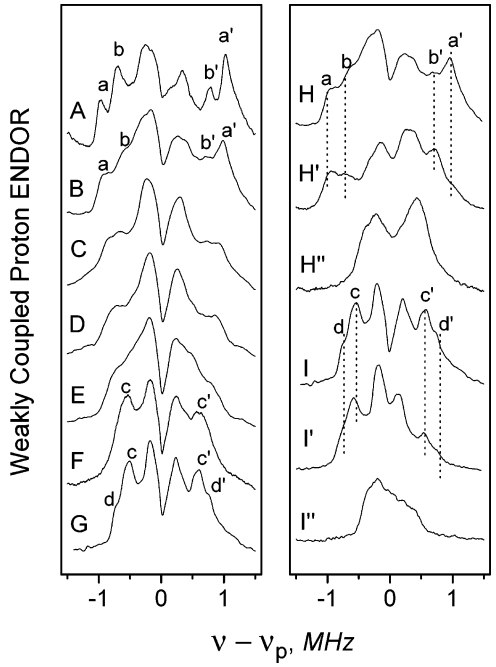

Figure 5. Spectra A−G present proton ENDOR from NO-Cyt *c*′ at the following magnetic fields: (A) 1.148 T ($g = 2.122$), (B)1.158 T ($g = 2.104$), (C) 1.178 T ($g = 2.069$), (D) 1.188 T ($g = 2.052$), (E) 1.198 T ($g = 2.034$), (F) 1.208 T ($g = 2.018$), and (G) 1.212 T ($g = 2.010$) to show the variation in frequencies across the EPR line shape of NO-Cyt *c*′. Spectra H, H′, H″−I, I′, I″ compare the weakly coupled proton ENDOR spectra of NO-Cyt *c*′ (H, I), Fe(OEP)NO (H′, I′), and Fe(TPP)NO (H″, I″) at 1.158 T ($g = 2.104$) (H, H′, H″) and 1.212 T ($g = 2.010$) (I, I′, I″) for the purpose of assigning meso-protons. The conditions for data collection were as follows: adiabatic rapid passage, $T = 2$ K, microwave power = 0.22 nW, 100 kHz field modulation = 0.5 G ptp, a system time constant = 160 ms, radio frequency power ≈ 20 W, radio frequency sweep rate = 0.15 MHz/s, overall signal averaging time = 500 s, $\nu_{EPR} = 34.10$ GHz. Radio frequency power was pulsed with a 100/900 μs duty cycle.

not well resolved, but its existence implies that there are exchangeable H/D having couplings less than the deuterium ENDOR line width of ∼0.5 MHz shown by the bar in the inset (where a deuterium coupling of 0.5 MHz would imply a coupling of 3.2 MHz for the corresponding proton). NO-Mb has shown quite different strongly coupled protons from those of NO-Cyt *c*′, and strong proton couplings of NO-Mb have been assigned by X-band ENDOR[29,31] to the distal imidazole and to the 6th liganding proximal histidine, neither of which exists for five-coordinate NO-Cyt *c*′.

Discussion

The molecular orbital model of five-coordinate NO-heme to which we refer is based on a semiquantitative description of pentacoordinate metal−NO complexes by Hoffmann and co-workers.[45] In this description a transition metal having four ligands, i.e., the ferroheme, bonds with NO. The d orbital configuration of a low spin ferroheme has filled $(d_{x^2-y^2})^2(d_{yz})^2(d_{xz})^2$ orbitals and empty (d_{z^2}) and (d_{xy}) orbitals. Note that the *x* and *y* axes for d orbitals are rotated 45° with respect to the to Fe−N axes of the heme; thus the d(*xy*) orbital is the sigma-bonding orbital pointing toward the heme nitrogens and the ($d_{x^2-y^2}$) orbital points at 45° with respect to the Fe−N axes of the heme. The NO electronic structure is "reduced to its essentials" (p 2667

(45) Hoffmann, R.; Chen, M. M. L.; Elian, M.; Rossi, A. R.; Mingos, D. M. P. *Inorg. Chem.* **1974**, *13*, 2666−2675.

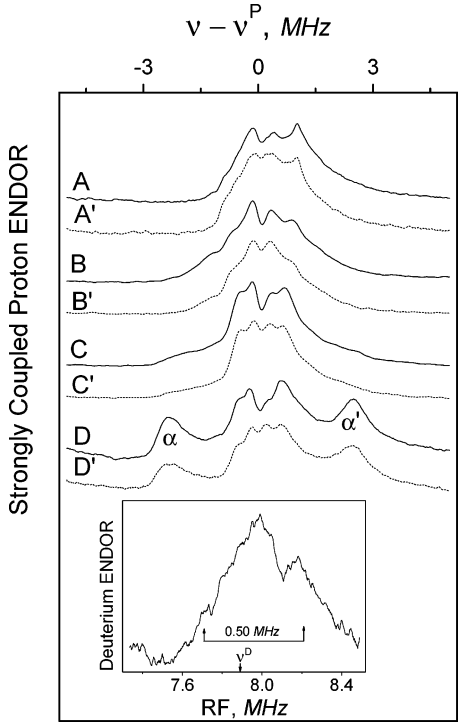

Figure 6. Spectra A−D (protonated solvent) and A′−D′ (deuterated solvent) are presented to show strongly coupled proton ENDOR from NO-Cyt *c*′ at respective fields of 1.158 T (g = 2.104) (A,A′), 1.188 T (g = 2.052) (B,B), 1.208 T (C,C′) (g = 2.018), and 1.212 T (g = 2.010) (D,D′). The conditions for proton data collection were as follows: adiabatic rapid passage, T = 2 K; microwave power = 0.22 nW; 100 kHz field modulation = 1.0 G ptp for spectra A,A′,B,B′,C,C′ and 2.0 G ptp for D,D′; a system time constant = 160 ms; radio frequency power ≈ 20 W; radio frequency sweep rate = 0.5 MHz/s; overall signal averaging time = 500 s; ν_{EPR} = 34.10 GHz. Radio frequency was pulsed with a 100/900 μs duty cycle. The inset is a deuterium ENDOR spectrum occurring near the free deuteron ENDOR frequency of 7.9 MHz at H = 1.208 T. The deuterium ENDOR conditions used were as follows: adiabatic rapid passage, T = 2 K; microwave power = 0.22 nW; 100 kHz field modulation = 0.15 G ptp; a system time constant = 320 ms; radio frequency power ≈ 20 W; radio frequency sweep rate = 0.06 MHz/s; overall signal averaging time = 1200 s; ν_{EPR} = 34.1 GHz. Radio frequency power was pulsed with a 100/900 μs duty cycle.

of ref 45), namely, the donor σ orbital, *n*, containing a somewhat delocalized lone pair of electrons on N and "that pair of superlative acceptor orbitals", the π^*_x and π^*_y orbitals, containing a total of one unpaired electron. Scheme 1 shows the basis orbitals and their energy levels: the d orbitals on the left, the NO orbitals on the right, the combined orbitals of the five-coordinate NO-heme with bent Fe−N−O in the center. In Scheme 1 the *x* and *y* subscripts at the NO orbitals indicate local NO axes that are generally different from those used by the d orbitals because NO does not bind axially. The energy of the π^* orbitals relative to the (d_{z^2}) orbital is a crucial matter, and the π^* orbitals are chosen to lie above the (d_{z^2}) orbital in energy[45] so that they can back-bond to (d_{yz}), (d_{xz}), and (d_{z^2}) orbitals. The *n* orbital containing the lone pair is chosen to lie below the metal d orbitals so that it will antibond to them. If FeNO were hypothetically arranged in a linear fashion along the *z* axis, the (d_{z^2}) orbital would antibond with the *n* orbital and the (d_{xz}) and (d_{yz}) orbitals would, respectively, back-bond with the π^*_x and π^*_y orbitals. A Walsh diagram (viz., Figure 3 of ref 45) shows that it is energetically favorable for such a pentacoordinate metal nitrosyl to have a bent rather than a linear FeNO bent configuration, consistent with the X-ray crystallographic structure.[17] For such a bent configuration we take, as shown in Scheme 2A, the *z* direction along the FeN bond of FeNO, the *x* direction in the FeNO plane perpendicular to the Fe−N bond, and the *y* direction normal to the FeNO plane. The upshot is that the energy separation of the (d_{z^2}) and the (d_{xz}) metal orbitals diminishes with an increasing Fe−NO bond angle, whereas the (d_{z^2}) and the (d_{yz}) metal orbitals continue to lie further from each other in energy. The energy of the (d_{xz}) orbital is raised with respect to the (d_{yz}) and (d_{xy}) orbitals by increased antibonding with the *n* orbital and diminished back-bonding with the π^*_x orbital. The energies of the (d_{yz}) orbital (normal to the FeNO plane) and of the nonbonding ($d_{x^2-y^2}$) orbital are relatively unchanged by the FeNO bending. When bending occurs, the energy of the (d_{z^2}) orbital is stabilized by back-bonding with the π^*_x orbital and by diminished antibonding with the *n* orbital. The $d_{x^2-y^2}$, d_{xz}, and d_{yz} orbitals each retain two electrons. The singly occupied molecular orbital (SOMO) ground state has primarily (d_{z^2}) character with some NO *n* and π^*_x character,[17,32] as shown in Scheme 2A. The SOMO accounts for hyperfine coupling to the NO and also, in combination with the energy levels of the (d_{xz}) and (d_{yz}) orbitals, accounts for the *g*-values of five-coordinate Fe−NO heme.

The *g*-Tensor. The *g*-tensor g_{max}, g_{inter}, g_{min} = 2.116, 2.017, 2.008 for the five-coordinate NO-heme complex can be explained with reference to the molecular orbital picture[45] described in the preceding paragraph and by Schemes 1 and 2A in which the (d_{z^2}) and the (d_{xz}) metal orbitals are brought close in energy by their interaction with the NO π^* and *n* orbitals. Spin−orbit coupling of the (d_{z^2}) component of the SOMO to the energetically near (d_{xz}) orbital causes g_y (g_y = g_{max} = 2.116 here) to differ the most from the free electron value of 2.00. This maximal *g*-tensor component was theoretically predicted and experimentally found from single crystals of Fe(OEP)(NO) to be perpendicular to the FeNO plane.[17,46] At room temperature g_{max} determined by single-crystal EPR lay within 9° of being perpendicular to the FeNO plane of Fe(OEP)(NO).[17] The direction for g_{max}, indicated by *y* in Scheme 2B, is a direction that points toward a set of diagonally opposite heme meso-protons because the FeNO plane at its lowest energy configuration overlays and bisects the pyrrole N−Fe−N 90° angle.[17] To first order, spin−orbit coupling of the (d_{z^2}) orbital in the SOMO orbital does not alter the *g*-value along the *z* direction normal to the heme shown in Scheme 2B. g_z should be closest to the free electron *g*-value of 2.00. The *g*-axis corresponding to the minimal *g*-value, as determined by single-crystal EPR study of Fe(OEP)(NO) at room temperature, lies within 2° of the normal to the heme and within 8° of the Fe−N direction.[17] Spin−orbit coupling of the (d_{z^2}) orbital to the energetically more distant metal (d_{yz}) orbital would cause the intermediate *g*-value, g_x, for NO-Cyt *c*′ to differ little from the free electron value.

Nitrogen Hyperfine Couplings. The results reported here provide definitive NO hyperfine couplings of a five-coordinate NO-hemeprotein for which binding of NO is intrinsic to function.[14,22] When NO binds in five-coordinate fashion to T hemoglobin,[28] NO is acting as an O_2 mimic, and there is spectral overlap of coexisting five- and six-coordinate NO-hemoglobin features. As shown by the comparison of ^{14}NO-Cyt *c*′ spectra with those of NO-Mb in Figure 4D−F (and with the NO

(46) Patchkovskii, S.; Ziegler, T. *Inorg. Chem.* **2000**, *39*, 5354−5364.

Scheme 1[a]

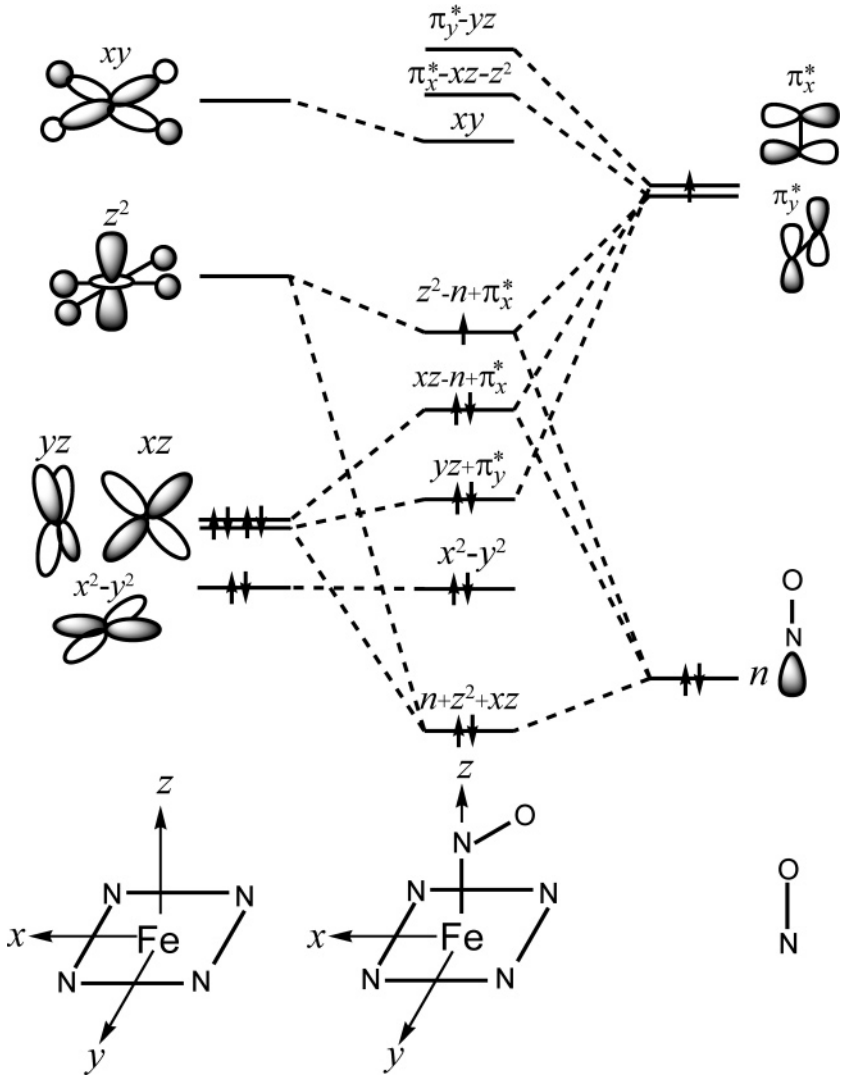

[a] Left: Energy levels, d orbitals, and spin population of the low spin d^6 ferroheme. Center: Perturbed d orbitals and wave functions after bonding to NO and bending of the FeNO. The lowest energy orbital has primarily *n* character, the next six orbitals, including the SOMO, have primarily d character, and the two highest unfilled energy levels have primarily π^* character. The energy levels are schematic. Right: Important orbitals of the nitrosyl ligand.

ENDOR of Fe(OEP)(NO) in the Supporting Information), the resolution of the NO hyperfine structure is considerably better from NO-Cyt *c*′, implying less randomness in the NO orientation and more precision in the binding of NO to Cyt *c*′. There are two NO conformers shown by X-ray crystallography of NO-Cyt *c*′,[7] rotated by 180° from one another, but one of the conformers appears to interact more strongly with positively charged Asp127. This interaction with Asp127 would render the structure of the two NO conformations electronically inequivalent. Since NO hyperfine structure is a measure of NO electronic structure, the implication of the excellent NO hyperfine resolution here may be that there is only one contributing NO conformer of NO-Cyt *c*′ at liquid helium temperature. Although there is some broadening of its ^{14}NO ENDOR features, the spectroscopic perturbation of the C-terminal his-tag to the five-coordinate NO-heme of Cyt *c*′ is a minor perturbation to EPR and ENDOR spectroscopy both here and previously.[22]

The ^{14}NO-Cyt *c*′ hyperfine couplings (Table 1), with a minimal value of 35.7 MHz and a maximal value of 43.7 MHz, are comparable to, although lower (as indicated by Figure 1S) than, the minimal and maximal couplings determined from single-crystal EPR of Fe(OEP)(NO), which were 40.9 and 49.7 MHz at room temperature and 42.5 and 52.8 MHz at 77 K. The minimal value of our ^{14}NO hyperfine coupling is at g_{max} (*y* direction in Scheme 2B). A minimal hyperfine interaction for ^{14}NO will occur in a direction perpendicular to the spin-containing 2p orbital contributed by the *n* and π^*_x of NO, and since the spin-containing 2p orbital (Scheme 2A) lies in the FeNO plane, the minimal hyperfine direction will be perpendicular to the FeNO plane in the direction of g_{max}. The quadrupolar coupling of $|P| = 0.67$ MHz measured at g_{max} is also consistent with the quadrupolar coupling measured perpendicular to the NO bond axis of NO.[47]

The maximal value of ^{14}NO hyperfine coupling is found at the high field, low *g*-value extremum of the EPR line shape at a minimal *g*-value for which the tensor direction would lie in the FeNO plane (Scheme 2B). This maximal hyperfine coupling would likely parallel the direction of the net, spin-containing 2p orbital, contributed by both the *n* and π^*_x orbitals of the NO. The overall ^{14}NO hyperfine tensor is largely isotropic with

(47) Dousmanis, C. *Phys. Rev.* **1955**, *97*, 967−970.

Scheme 2[a]

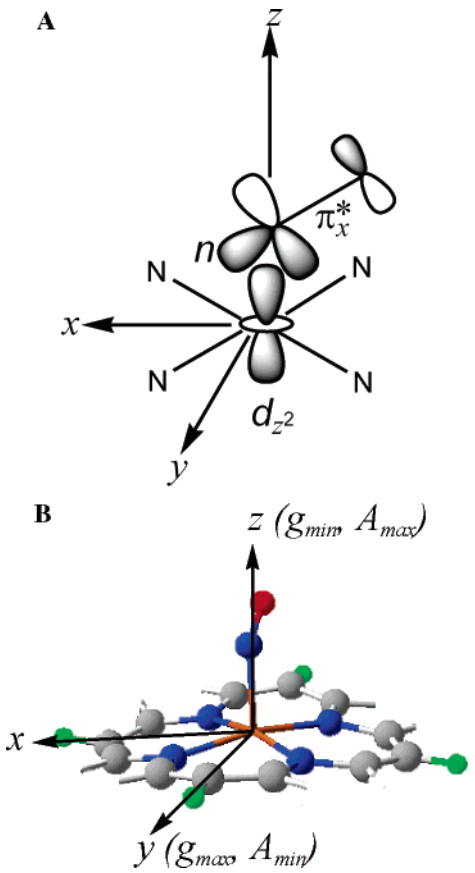

[a] (A) Molecular orbital of the SOMO which contains metal (d_{z^2}) and NO *n* and π^*_x contributions. The FeNO plane contains the *z* axis at or near the Fe−N bond normal to the heme. The *x* direction is in the FeNO plane perpendicular to the *z* direction. The *y* direction is perpendicular to the FeNO plane. (B) The configuration of the NO-heme, showing *x*, *y*, and *z* axes. The *y* axis is normal to the FeNO plane and is the direction for g_{max}, minimal NO hyperfine coupling A_{min}, and maximal meso-proton hyperfine coupling. The *xz* plane is the FeNO plane. The *z* direction normal to the heme is the direction of g_{min}, maximal NO hyperfine coupling A_{max}, and minimal meso-proton hyperfine coupling. The *x* axis is associated with the intermediate *g*-value.

an average isotropic coupling of 39.7 ± 0.4 MHz, and this means that there is considerable s character to the unpaired spin on the NO. If this s character were entirely valence 2s character, the spin-containing molecular orbital on NO would have 2.5% 2s character,[48] where this 2s character arises from the NO *n* orbital (Schemes 1 and 2A). The total variation of 8.0 MHz in the ^{14}NO hyperfine constant, if entirely 2p in character, represents 5.2% 2p character.[49] Thus the 2:1 2p-to-2s ratio observed by ENDOR is an effect of simultaneous bonding of the sp (*n*) and p (π^*_x) orbitals of NO with the (d_{z^2}) of the Fe as shown in Scheme 2A. Recent DFT calculations show the overall spin density on the nitrogen to be similar to that which we empirically estimate, with a prediction of ≤10% total spin on the NO.[17,32,50] Six-coordinate Fe-NO-heme systems such as NO-Mb and NO-cytochrome *c* oxidase have a ∼4-fold greater NO hyperfine anisotropy (of ∼30 MHz). This greater anisotropy implies a ∼4-fold larger 2p electron spin density and more π^*_x character in the SOMO. An underlying reason for having more NO π^*_x character associated with the six-coordinate NO-heme-His system is that the antibonding sigma interaction of the His nitrogen with the (d_{z^2}) orbital raises the energy of the (d_{z^2}) orbital closer to the energy of the π^*_x orbital (see Scheme 1) and leads to a stronger back-bonding contribution of the π^*_x orbital in the SOMO.

The small nitrogen feature near 6 MHz in the ENDOR spectra of Figure 3 is assigned to the heme nitrogen, and the hyperfine coupling to this $^{14}\nu^+_{ENDOR}$ feature is about 4.5 MHz. ESEEM (Electron Spin−Echo Envelope Modulation) and associated HYSCORE (Hyperfine Sublevel Correlation Spectroscopy) measurements of the heme nitrogen hyperfine couplings in five- and six-coordinate NO ferrous porphyrin complexes have provided heme nitrogen hyperfine couplings of the order of 5 MHz.[34,51,52]

Proton ENDOR. A. ENDOR of Weakly Coupled Meso-Protons. The assignment of meso-proton ENDOR peaks was carried out by a comparison of proton ENDOR from Fe(OEP)(NO), which has meso-protons, and from Fe(TPP)(NO) which lacks them. All other outlying porphyrin protons which are further from the heme iron have smaller couplings than the meso-protons, notably, smaller point dipolar couplings (eq 3) to the electron spin on the heme iron. We have determined from high,[53] low,[21] and intermediate[22] spin ferric heme systems that the majority of the meso-proton coupling is point dipolar coupling (eq 3) to the electron spin on the heme iron, where most of the unpaired electron spin resides. For the five-coordinate NO-heme system, it appears from the NO hyperfine coupling and from theory[17,32,50] that the majority (∼90%) of the spin in the SOMO is in the metal (d_{z^2}) orbital. From the crystallographic 3.4 Å iron-to-meso-carbon distance plus an additional 1.1 Å CH bond, we estimate a 4.5 Å distance (*R* in eq 3) from the iron-to-meso-proton. Then the point dipolar coupling from spin localized on the iron provides a first approximation for calculating the meso-proton hyperfine coupling via eq 3 with $f_{Fe} = 0.9$. For measurements done at g_{max} we take $g_{eff} \approx 2.122$ in eq 3. The maximal meso-proton point dipolar contribution to eq 3 should be $2A_{PTdip} = (+)1.7$ MHz when the magnetic field is along the direction from the iron to a meso-proton ($\theta = 0°$ in eq 3 where the axis labeled "3" in eq 2 is along the iron-to-meso-proton vector). Smaller dipolar couplings, $(-)A_{PTdip}$ of approximately (−)0.80 MHz, will occur when the magnetic field is perpendicular to the direction from the iron to a meso-proton (i.e., $\theta = 90°$ in eq 3, corresponding to the axes labeled "1" or "2" in eq 2.)

(48) The Fermi coupling in MHz is related to the fraction of unpaired spin in a 2s orbital as follows: $A_{Fermi} = (16 \times 10^{-6}) f_{2s} g_n \beta_e \beta_n |\psi_{o2s}|^2 \pi/(3h) = (1.59 \times 10^3) f_{2s}$ (MHz), where f_{2s} is the fraction of unpaired electron spin in the nitrogen 2s orbital, g_n is the ^{14}N nuclear *g*-value (= 0.403 47), β_e and β_n are the electron and nuclear Bohr magnetons, $|\psi_{o2s}|^2 = 33.4 \times 10^{24}$ cm^{-3} (Hartree, D. R.; Hartree, W. *Proc. R. Soc. London, Ser. A* **1949**, *193*, 299−304.) is the 2s wave function at the nitrogen nucleus, and *h* is Planck's constant.

(49) The anisotropic contribution from a 2p electron is related to the fraction of unpaired spin in that orbital as follows: $A_p = (4 \times 10^{-6}) f_{2p} g_n \beta_e \beta_n \langle r^{-3} \rangle_{2p} / (5h) = (48.1) f_{2p}$ (MHz), where f_{2p} is the fraction of unpaired electron spin in a particular nitrogen 2p orbital, $\langle r^{-3} \rangle_{2p} = 21.1 \times 10^{24}$ cm^{-3} (Hartree, D. R.; Hartree, W. *Proc. R. Soc. London, Ser. A* **1949**, *193*, 299−304.) is the expectation value of r^{-3} for a nitrogen 2p orbital, and *h* is Planck's constant. The maximum anisotropic difference between orientations parallel and perpendicular to the direction of the 2p orbital would be $3A_p = 144.9$ MHz.

(50) Zhang, Y.; Mao, J.; Godbout, N.; Oldfield, E. *J. Am. Chem. Soc.* **2002**, *124*, 13921−13930.
(51) Tyryshkin, A. M.; Dikanov, S. A.; Reijerse, E. J.; Burgard, C.; Huettermann, *J. Am. Chem. Soc.* **1999**, *121*, 3396−3406.
(52) Gilbert, D. C.; Dikanov, S. A.; Doetschman, D. C.; Smeija, J. A. *Chem. Phys. Lett.* **1999**, *315*, 43−48.
(53) Mulks, C. F.; Scholes, C. P.; Dickinson, L. C.; Lapidot, A. *J. Am. Chem. Soc.* **1979**, *101*, 1645−1654.

The largest experimental magnitude at any *g*-value for meso-proton hyperfine coupling was 1.9 ± 0.2 MHz shown by the features **a,a′** at $g_{max} = 2.122$ (Figure 5A). This largest magnitude meso-proton coupling occurred at the maximal *g*-value (*y* axis in Scheme 2B) for which the direction is perpendicular to the FeNO plane.[17,46] Thus the directions coincide for g_{max} perpendicular to the FeNO plane and for the maximum meso-proton dipolar coupling. That means the proton tensor direction for A_3 (i.e., the axis "3" in eq 2) coincides with the direction of g_{max}. The implication is that the FeNO plane bisects the heme N−Fe−N 90° angle so that the direction for g_{max}, which is perpendicular to the FeNO plane, points along the Fe-to-meso-proton vector. At the same extremal g_{max} there is another set of proton features, **b,b′** (Figure 5A), which we also assign to meso-protons, and their coupling is 1.5 ± 0.2 MHz. This coupling should arise from the other set of diagonally opposite meso-protons for which the field is perpendicular to the vector from Fe to them. At g_{max} the meso-proton point dipolar coupling at the $\theta = 90°$ extremum is calculated as $-A_{PTdip} = (-)0.85$ MHz. This coupling would occur along an axis which we designate axis "2" in eq 2, an axis perpendicular to the Fe-to-meso-proton direction and approximately in the heme plane. If dipolar coupling dominates, the sign of the tensor component for A_2 should be negative. Next, all of the meso-protons should experience a minimal value to their dipolar hyperfine coupling when the magnetic field is simultaneously perpendicular to the heme and perpendicular to all meso-proton-to-Fe vectors (i.e., $\theta = 90°$ in eq 3, corresponding to axis "1" in eq 2). The features **c,c′** of Figure 5F and G at $g = 2.01$ with experimentally measured coupling of 1.2 ± 0.1 MHz presented such a minimal value in meso-proton couplings. At $g_{min} \approx 2.01$ the meso-proton point dipolar value for the $\theta = 90°$ extremum was calculated as $A_{PTdip} = (-)0.8$ MHz. Electronic *g*-values near 2.00 are in the FeNO plane,[17,46] which happens to be perpendicular to the direction for g_{max}. The minimal meso-proton hyperfine coupling occurs within 0.01 unit of the minimal *g*-value.[54] Thus the axis which we designate axis "1" in eq 2 is an axis perpendicular to the Fe-to-meso-proton bond and to the heme plane. If dipolar coupling dominates, the sign of the tensor component for A_1 should be negative. Although we have not explicitly determined the angular orientation of axis 3 with respect to the $g_{min}-g_{inter}$ tensor directions by angle-selected ENDOR,[41,55−58] the minimal meso-proton hyperfine coupling should and does occur very near the minimal *g*-value and it will occur normal to the heme.

The maximal and minimal meso-proton hyperfine extremal couplings and the *g*-values at which they were measured provide information on the orientation of the FeNO plane with respect to the heme (and *vice versa*). Before analyzing the meso-proton hyperfine tensor, we provide explanation here for the potential covalent contributions to that tensor. For the meso-proton, which is an "α-proton" with respect to its adjacent meso-carbon, a covalent contact interaction contribution to a_{iso} of eq 2 can arise by exchange polarization of the adjacent pπ spin density on the meso-carbon (see pp 81−83 of ref 43) or by direct spin transfer from the Fe through the sigma porphyrin skeleton. a_{iso} from pπ spin polarization would be negative while a_{iso} from sigma transfer would be positive.[59] The strength of the pπ contact interaction is proportional to the pπ spin density on the meso-carbon through a McConnell relation, a_{iso} (MHz) $\approx (-60)\rho_C$ (see p 4534 of ref 59), where ρ_C is the fraction of pπ spin on the adjacent meso-carbon. There may be a small anisotropic covalent dipolar contribution as well to the dipolar coupling from pπ spin on the meso-carbon. As explained in pp 103−107 of ref 43, these dipolar couplings to pπ spin on the meso-carbon will be positive with coupling $\approx +30\rho_C$ along the C−H bond direction, ≈0 along the heme normal, and negative with coupling $\approx -30\rho_C$ in a direction perpendicular to the C−H bond in the heme plane.

To obtain an estimate of the overall meso-proton hyperfine tensor from the features, **a**,**a′**, **b**,**b′**, and **c**,**c′**, we make the assumption that the hyperfine tensors of the heme meso-protons are related by the 4-fold symmetry of the heme. (Features **b**,**b′** as measured at g_{max} actually belong to different hemes from the features **a**,**a′**). Estimates of the hyperfine tensor from eq 2 become: $A_1 = T_1 + a_{iso} = (-)1.2 \pm 0.1$ MHz, $A_2 = T_2 + a_{iso} = (-)1.5 \pm 0.2$ MHz, $A_3 = T_3 + a_{iso} = (+)1.9 \pm 0.2$ MHz. The result is that $a_{iso} = (-)0.27 \pm 0.1$ MHz, $T_1 = (-)0.93 \pm 0.2$ MHz, $T_2 = (-)1.23 \pm 0.2$, $T_3 = (+)2.16 \pm 0.2$. The negative isotropic contribution of (−)0.27 MHz would imply that about 0.5% unpaired electron spin arrives at the meso-carbon pπ orbital.[60] The anisotropic tensor components, T_1, T_2, and T_3, are largely but not fully explained by point dipolar contributions, which would respectively be (−)0.8, (−)0.85, and (+)1.7 MHz. Even if one includes the anisotropic local dipolar interaction proportional to ρ_C,[43] one adds only about −0.13 MHz to T_2 and +0.13 MHz to T_3, thus predicting $T_1 = (-)0.80$, $T_2 = (-)0.98$, and $T_3 = (+)1.83$ MHz. The predicted magnitudes of T_1, T_2, and T_3 are, respectively, ∼20% smaller than (−)0.93, (−)1.23, (+)2.16,[61] although the conclusion still holds that the anisotropic part of the meso-proton dipolar interaction shows the orientation of the heme and its meso-protons with respect to the FeNO plane. One reason the predicted magnitudes of

(54) At the extreme high field edge of the EPR line shape (Spectrum 5G) the shoulder (**d,d′**) emerged, and it is thus plausible that the tensor direction for the lowest *g*-value has tilt with respect to the heme normal in the FeNO plane. Since there is also evidence for these shoulders (**d,d′**) from Fe(OEP)(NO), their existence appears intrinsic to an Fe(heme)(NO) having meso-protons and is not due to interaction with the protein environment.

(55) Hoffman, B. M.; Martinsen, J.; Venters, R. A. *J. Magn. Reson.* **1984**, *59*, 110−123.

(56) Hoffman, B. M.; Venters, R. A.; Martinsen, J. *J. Magn. Reson.* **1985**, *62*, 537−542.

(57) Hoffman, B. M.; Gurbiel, R. J. *J. Magn. Reson.* **1989**, *82*, 309−317.

(58) Detailed angle-selected ENDOR simulations near g_{min} (after refs 55−57) are complicated by loss of orientation selectivity due to nearly equal values of g_{min} and g_{inter}, to *g*-strain, and to significant nitrogen hyperfine coupling. All of these complications serve to broaden the ENDOR pattern. GENDOR (ref 57) spectral simulations based on $A_1 = (-)1.2$, $A_2 = (-)1.5$, $A_3 = (+)1.9$ MHz for the meso protons and with 30−60 G EPR line broadening showed in the $g_{min}-g_{inter}$ range two broad proton hyperfine peaks separated by about 1.2 MHz.

(59) Walker, F. A. *Inorg. Chem.* **2003**, *42*, 4526−4544.

(60) We suggest that the mechanism that permits electron spin to be transferred to the meso-protons is overlap of the $d(z^2)$ orbital with the porphyrin a_{2u} (π) orbital, an overlap which, in the case of high and intermediate spin ferric hemes (Cheng, R.-J.; Chen, P.-Y. *Chemistry—A European Journal* **1999**, *5*, 1708−1715. Cheng, R.-J.; Chen, P.-Y.; Lovell, T.; Liu, T.; Noodleman, L.; Case, D. A. *J. Am. Chem. Soc.* **2003**, *125*, 6774−6783. Walker, F. A. *Inorg. Chem.* **2003**, *42*, 4526−4544. Usov, O. M.; Choi, P. S.-T.; Shapleigh, J. P.; Scholes, C. P. *J. Am. Chem. Soc.* **2005**, *127*, 9485−9494.), required iron out-of-planarity. The Fe of NO-Cyt *c′* is 0.31 Å out of the average pyrrole nitrogen plane toward the NO ligand (Lawson, D. M.; Stevenson, C. E.; Andrew, C. R.; Eady, R. R. *EMBO J.* **2000**, *19*, 5661−5671.); whereas the iron out-of-planarity for ferric Cyt *c′* is 0.25 Å (Ramirez, L. M.; Axelrod, H. L.; Herron, S. R.; Rupp, B.; Allen, J. P.; Kantardjieff, K. A. *Journal of Chemical Crystallography* **2003**, *33*, 413−424.)

(61) If we consider a simpler axial meso-proton hyperfine interaction with $A_1 = (-)1.2 \pm 0.1$ MHz and $A_3 = T_3 + a_{iso} = (+)1.9 \pm 0.2$ MHz, we can estimate a_{iso}, T_1, and T_3. The estimate is $a_{iso} = (-)0.17$, $T_1 = (-)1.04$, and $T_3 = (+)2.07$ MHz, values which still show pπ spin density on the meso-carbon and a ∼20% larger anisotropic coupling than predicted by the point dipolar interaction.

T_1,T_2,T_3 may be too small is that spin distributed throughout the heme and NO, not just to Fe, should be considered in calculating dipolar interactions and exchange polarization effects. Additionally, in our analysis we have taken the four meso-protons as electronically equivalent by 4-fold heme symmetry. It is possible that the electronic asymmetry induced by the bent FeNO configuration propagates to the heme periphery and renders the meso-protons electronically inequivalent. To answer both of these concerns, higher level theory (DFT) should help in estimating overall delocalized spin and electronic inequivalence.[32,50,62]

B. ENDOR of Strongly Coupled Protons. The nearest strongly coupled protons elucidated from the previous ENDOR study on ferric *R. sphaeroides* Cyt *c′* were those on Phe14. Their couplings of about 3.5 MHz were dipolar in character, after eq 3. That dipolar coupling corresponded to a calculated distance from the iron to a Phe14 ring proton of 3.5 Å.[22] Using the coordinates of Phe14 from ferric *R. sphaeroides* Cyt *c′* superimposed on the coordinates of NO-Cyt *c′* of *A. xylosoxidans*, we estimated distances of the nearest protons on the Phe14 ring at 3.0 and 3.3 Å from the heme iron. The closest proton of Phe14, as determined from the estimate (via Swiss PdB Viewer) of the dihedral angle between the planes determined by the atoms Fe−N−O and Fe−N−H, lay in the Fe−N−O plane for the NO shown in Figure 1. If the relevant H, Fe, N, and O all lie within the same plane, this would mean that the Fe−H vector lies within the $g_{inter}-g_{min}$ plane and can achieve its maximal, best resolved ENDOR coupling at the high field, minimal *g*-value extremum of the EPR line shape, as indeed the proton features, α,α′, shown in Figure 6 D do. Its coupling of 4.7 MHz ($= 2A_{PTdip}$ in eq 3) would imply that the Fe−proton distance is 3.1 Å when g_{min} is aligned along the Fe−proton vector for this proton if 90% of the spin is on the Fe. The above considerations provide strong evidence that the proton observed by ENDOR in Figure 6D is from the occluding Phe14. In the absence of structural evidence to the contrary, it had not been ruled out that the five-coordinate NO of some NO-Cyts *c′* could be on the distal side (i.e., the Phe14 side) of the heme.[63] If this were the case, we would expect that the conformation of Phe14 would be markedly perturbed from its position in the absence of NO, and our proton ENDOR results indicate that it is not perturbed. The NO that we study here is thus on the expected proximal side of the heme where it has replaced the proximal histidine.

Two of the Arg127 side chain protons are within less than 2.5 Å of the O in the NO orientation of Figure 1. Thus it is conceivable that these protons could provide proton hyperfine coupling if there were adequate spin density on the O. However, these protons respectively lie 4 Å and 5 Å from the iron, which is the main source of electron spin.[17] The dipolar coupling to spin on the Fe would be less than 3 MHz for a proton 4 Å distant. These protons also appear to lie away from any of the *g*-tensor axes, since they lie well out of the plane determined by FeNO and well off the normal to the FeNO plane. The nearest exchangeable water is 5.5 Å distant[18] and would have a maximum proton coupling < 1 MHz. We did see evidence for exchangeable proton broadening of the NO-Cyt *c′* ENDOR in Figure 6, but our perception is that the exchangeable proton coupling is less than 4 MHz. To better delineate the possible exchangeable proton/deuteron coupling, we presented the deuterium ENDOR, where the width of the deuterium ENDOR (Inset to Figure 6) is ≤0.5 MHz. A deuterium coupling of ≤0.5 MHz would correspond to a proton coupling of ≤3.2 MHz. Our conclusion is that the exchangeable deuteron couplings are from the exchangeable deuterons of Arg127. Their unresolved ENDOR character implies that they lie out of the FeNO plane and well off the normal to the FeNO plane. There may be disorder in the position of the exchangeable H/D of Asp127, consistent with the theoretical findings on the lack of importance of Arg to establishing the free energy that favors NO 5-coordination.[64]

Admixture of Six-Coordinate NO-Cyt c′. A six-coordinate NO-heme-His intermediate has been proposed as a transient predecessor to the final five-coordinate NO-Cyt *c′* species of *A. xylosoxidans*.[8,64−67] A recent report indicates that the NO-Cyt *c′* of *R. capsulatus* develops comparable percentages of six-coordinate and five-coordinate NO species; in some NO-Cyt *c′* complexes there can be six-coordinate NO-heme-His species present under equilibrium conditions. [63] Cyt *c′* of *R. capsulatus* has an occluding phenylalanine like that of *R. sphaeroides* Cyt *c′*, and it has a solvent accessible distal coordination site. Occasional samples of *R. sphaeroides* NO-Cyt *c′* showed a small fraction of six-coordinate signal with EPR intensity at high fields below $g = 2.00$ like that of six-coordinate NO-Mb; the six-coordinate fraction was estimated as 10% from comparison with integrated NO-Mb and five-coordinate NO-Cyt *c′* signals. A comparison of nitrogen ENDOR was made at $g = 1.985$ from the six-coordinate signals of NO-Mb and six-coordinate NO-Cyt *c′*, and this comparison is shown in the Supporting Information (Figure 2S). Both samples showed the characteristic sharp histidine ENDOR feature near 12 MHz and a broader higher frequency ^{14}NO feature near 20 MHz. Interestingly, the histidine hyperfine coupling constant was notably larger for the six-coordinate NO-Cyt *c′* than for NO-Mb by approximately 2 MHz, and the ^{14}NO coupling is smaller by several MHz. This difference may signify, on comparison with NO-Mb, a stronger Fe−His ligation for six-coordinate NO-Cyt *c′* and a weaker Fe−NO bond, consistent with the predicted destabilization of six-coordinate NO-Cyt *c′*.[64] In a preliminary study, we have determined that the percentage contribution of six-coordinate NO-Cyt *c′* can be enhanced by preparation of NO-Cyt *c′* through stoichiometric addition of NO, rather than by addition of NO in excess, as was done to make five-coordinate NO-Cyt *c′*.

Conclusions

The nitrogen ENDOR taken over the entire *g*-value range showed the NO nitrogen hyperfine coupling to be predominately isotropic. The maximum value of this hyperfine coupling occurred at electronic *g*-values near 2.00 for which the tensor directions lie in the FeNO plane, a plane in which the NO π_x and *n* electrons indicated in Schemes 1 and 2 reside. The unpaired electron on N, as judged from its large contact

(62) Mao, J.; Zhang, Y.; Oldfield, E. *J. Am. Chem. Soc.* **2002**, *124*, 13911−13920.
(63) Andrew, C. R.; Kemper, L. J.; Busche, T. L.; Tiwari, A. M.; Kecskes, M. C.; Stafford, J. M.; Croft, L. C.; Lu, S.; Moenne-Loccoz, P.; Huston, W.; Moir, J. W.; Eady, R. R. *Biochemistry* **2005**, *44*, 8664−8672.
(64) Marti, M. A.; Capece, L.; Crespo, A.; Doctorovich, F.; Estrin, D. A. *J. Am. Chem. Soc.* **2005**, *127*-.
(65) George, S. J.; Andrew, C. R.; Lawson, D. M.; Thorneley, R. N.; Eady, R. R. *J. Am. Chem. Soc.* **2001**, *123*, 9683−9684.
(66) Andrew, C. R.; George, S. J.; Lawson, D. M.; Eady, R. R. *Biochemistry* **2002**, *41*, 2353−2360.
(67) Andrew, C. R.; Rodgers, K. R.; Eady, R. R. *J. Am. Chem. Soc.* **2003**, *125*, 9548−9549.

component, appears to have sp^n character with $n \approx 2$, and not π^* character lacking s admixture. If the unpaired valence electron has an admixture of valence 2s and 2p wave functions, on the NO nitrogen there is 7.7% of an electron spin with 2.5% 2s character and 5.2% 2p character. The percentage of unpaired 2p spin for the NO nitrogen of five-coordinate NO-Cyt *c*′ is considerably less than the percentage of unpaired 2p spin of six-coordinate NO-Mb. There was additional evidence for a smaller hyperfine coupling to the heme nitrogen with coupling of the order 4.5 MHz.

The proton couplings determined here gave information on the electronic structure of the NO-heme complex and on the physical proximity of conserved amino acid side chains.

(1) ENDOR frequencies from heme meso-protons, assigned with reference to porphyrin models, were determined to arise from an anisotropic hyperfine interaction. The largest magnitude of meso-proton dipolar coupling occurred at g_{max}, for which the tensor direction is known to be perpendicular to the FeNO plane.[17,46] The largest magnitude of meso-proton hyperfine dipolar coupling will occur for an orientation of the magnetic field along the Fe−meso-proton direction. Thus the perpendicular to the FeNO plane and the direction pointing from the Fe toward heme meso-protons coincide. The conclusion is that the FeNO plane bisects the heme N−Fe−N 90° angle so that g_{max} points toward meso-protons. Meso-proton hyperfine coupling of minimal magnitude should occur when the magnetic field is perpendicular to the heme, and the minimal coupling did occur at a *g*-value close to 2.00. The axis corresponding to such an electronic g-value is expected to lie in the FeNO plane.[17,46] Thus the normal to the heme is in the FeNO plane lying close to the Fe−N bond direction. The overall meso-proton hyperfine tensor was interpreted to show possible evidence for a negative meso-proton Fermi contact interaction brought on by unpaired electron spin density in their adjacent meso-carbon pπ orbitals.

(2) There was a well resolved proton coupling which is assigned with confidence to the nearest proton of the Phe14 side chain. Superposition of the Phe14 structure from *R. sphaeroides* ferric Cyt *c*′ on to the NO-heme structure from *A. xylosoxidans* provided a prediction of a 3.0 Å distance of the nearest Phe14 proton from the heme iron and appropriately predicted that this nearest proton would be in the plane determined by Fe, N, and O of FeNO (a plane which also happens to be the $g_{inter}-g_{min}$ plane). The hyperfine coupling to this proton was largest and best resolved at g_{min}. The magnitude of this coupling, if due to a point dipolar interaction with the Fe (eq 3), predicted the proton to lie 3.1 Å from the Fe. The position of the Phe14 side chain is little perturbed in NO-Cyt *c*′ from its position in ferric Cyt *c*′.

(3) Deuterium ENDOR provided evidence of a nearby exchangeable proton(s) consistent with the side chain protons of Arg127 that could hydrogen bond to the NO ligand.[7]

Acknowledgment. These studies were partially supported by the NIH (EB00326929, C.P.S.) and the DOE (95ER20206, J.P.S.). We are grateful to Dr. Mark Nilges, Department of Chemistry, University of Illinois, for providing the SIMPIPM EPR spectral simulation and fitting program.

Supporting Information Available: The following figures: Figure 1S, which is a comparison of nitrogen ENDOR from Fe(OEP)(NO) and ^{14}NO-Cyt *c*′ at a magnetic field of 1.178 T ($g = 2.069$); Figure 2S, which compares nitrogen ENDOR from six-coordinate ^{14}NO-Cyt *c*′ and ^{14}NO-Mb at a magnetic field of 1.227 T below $g = 2.00$ ($g = 1.985$). This material is available free of charge via the Internet at http://pubs.acs.org.

JA055323F